Probing Rapid Ion Transfer Across a Nanoscopic Liquid−Liquid Interface

Chenxin Cai,[†] Yuehong Tong, and Michael V. Mirkin*

Department of Chemistry and Biochemistry, Queens College−CUNY, Flushing, New York 11367

Received: August 16, 2004; In Final Form: September 7, 2004

Rapid kinetics of tetraalkylammonium ion transfers (ITs) across the interface between water and 1,2-dichloroethane was measured by steady-state voltammetry at nanometer-sized pipet electrodes (with an orifice radius of 10−300 nm). Methodologies previously used for preparation and characterization of micrometer-sized pipets are shown to be suitable for experiments with nanopipets. The silanization of the outer pipet wall results in quantitative agreement between the experimentally measured and theoretically predicted values of the diffusion-limiting current to the pipet. An independent estimate of the orifice radius and the thickness of the glass wall were obtained by using a nanopipet as a scanning electrochemical microscopy (SECM) tip. The voltammograms of IT from the outer solution into the pipet and from the filling solution out of the pipet were analyzed to measure rates of both forward and reverse IT reactions (i.e., from water to organic and from organic to water). The measured standard rate constants are compared with the values predicted by the theory. The effects of the pipet geometry and silanization on the shape of voltammograms and the magnitude of the apparent IT rate constant are discussed.

Introduction

Several theoretical and experimental studies of ion transfer (IT) reactions at the interface between two immiscible electrolyte solutions (ITIESs) have been performed over the last three decades.[1] IT processes are of great fundamental interest; they are also relevant to many important biological and technological systems, from chemical sensors to drug delivery systems in pharmacology to biological membranes.[2] Several theoretical treatments of IT reactions at the ITIES have been published.[3−9] Those treatments are based on completely different (and sometimes conflicting) models. Typically, the finite rate of the interfacial IT is attributed either to the existence of an activation barrier[3,4] or to slow diffusion of the transferred species through the mixed interfacial layer.[5,6] Marcus[7] combined the idea of slow ionic diffusion across the phase boundary with the possibility of an activation barrier to the change of solvation. His model also accounts for the effect of ''fingers" (i.e., protrusions of one solvent into another solvent predicted by computer simulations[8]) on the solvation/desolvation of transferred ions.

The presently available experimental data do not allow one to differentiate between the conflicting models. Despite being conceptually different, those theories predict surprisingly similar current−potential curves. Moreover, there are concerns that most rate constants measured for rapid IT reactions at macroscopic (e.g., mm-sized) ITIES were affected by uncompensated ohmic resistance and capacitive current.[1a,1d,7] To minimize those effects, Girault's group introduced micro-ITIES, which can be formed either at the tip of a pulled glass micropipet or within a small hole made in a thin membrane.[10] Although several groups reported kinetic measurements at micro-ITIES,[1d] most IT reactions have turned out to be too fast to be probed at micrometer-sized interfaces under steady-state conditions.[11,12] The higher steady-state mass-transfer rates could be achieved either by using nanopipets[12] or by doing measurements in a submicrometer-thick gap between a pipet used as a tip in the scanning electrochemical microscope (SECM) and a macroscopic ITIES.[13]

In this paper, we report kinetic measurements of tetraalkylammonium IT between 1,2-dichloroethane (DCE) and water phases. The transfers of tetraethylammonium (TEA^+) and tetramethylammonium (TMA^+) ions between DCE or nitrobenzene and water are perhaps the most-popular model experimental systems used for checking the IT theory. These reactions are among the fastest known IT processes. They have been extensively studied during several decades,[1,14−18] and the reported standard rate constants ($k°$) varied from 10^{-3} cm/s to 1 cm/s. As expected, the rate constants measured at micro-ITIESs were generally higher than the results obtained at macroscopic interfaces, which were affected by ohmic potential drop (*iR*-drop) in the resistive organic phase. However, the $k°$ values of 0.20 and 0.12 cm/s (for TEA^+ and TMA^+, respectively) measured by cyclic voltammetry at the macroscopic DCE/water interface[18] were comparable to the values obtained at the micro-ITIESs. The measurements at microscopic interfaces may suffer from poor characterization of the interfacial geometry and edge effects.[19] The *iR*-drop compensation, which may still be required for pulse and AC techniques,[20] and the intricacy of impedance analysis at micro-ITIESs also may have affected the determined rate constants.[21]

The negligibly small *iR*-drop across nano-ITIESs (<1 mV) and very straightforward data analysis suggest that steady-state nanopipet voltammetry may be less affected by experimental problems than the measurements at larger interfaces. The consistent rate constant values were obtained previously for rapid transfers of potassium[12a]

$$K^+(w) + DB18C6\,(DCE) \rightleftarrows [K^+DB18C6]\,(DCE) \quad (1)$$

and other alkali-metal ions[12b] facilitated by dibenzo-18-crown-6, using a broad range of nanopipet radii (e.g., 5−250 nm[12a]). Here, we will use the facilitated potassium transfer as a model reaction to perform a complete characterization of the pipet

* Author to whom correspondence should be addressed. Telephone: 718-997-4111. Fax: 718-997-5531. E-mail address: Michael_Mirkin@qc.edu.

[†] Permanent address: Department of Chemistry, Nanjing Normal University, Nanjing 210097, Jiangsu Province, PRC.

10.1021/jp046304f CCC: $27.50
Published on Web 10/26/2004

geometry and mass transfer, including the effects of silanization, and of the finite thickness of the pipet wall. It was found earlier[17] that a hydrophilic outer wall of a glass pipet immersed in organic solvent retains a submicrometer-thick aqueous layer. This layer increases the apparent interfacial area and results in a diffusion current value that is significantly larger than the theoretical value, based on the pipet radius. For micrometer-sized pipets, an aqueous film could be eliminated by silanizing the outer pipet wall, to render it hydrophobic.[19] However, the possibility and effectiveness of nanopipet silanization has not yet been documented. According to ref 12b, the silanization of nanopipets is very difficult, whereas in ref 13e, only relatively large (radius of 300−450 nm) pipets were determined to be suitable for silanization.

Another factor that affects the mass transfer to a pipet is the thickness of its wall. When the wall is thin, the additional diffusion flux from the back of the pipet can increase the limiting current by >30%.[13b,22] For micrometer-sized pipets, the glass thickness can be determined microscopically. It was also shown that the ratio of the glass wall radius to the orifice radius (RG $= r_g/a$) can be evaluated using the pipet as an SECM tip.[13b,23] In those experiments, the voltage was applied between the reference inside the pipet and the external organic reference electrode to induce the IT reaction (e.g., see reaction 1). The tip current was limited by diffusion of DB18C6, and it decreased when the tip was brought close to a solid substrate, which blocked the diffusion of DB18C6 to the pipet orifice (negative feedback). A reliable RG value for a micrometer-sized pipet could be obtained by fitting the current−distance (i_T vs d) curves to the available theory. Here, we show that this approach can be used to characterize the geometry of nanopipets.

An important feature of a facilitated IT process (1) is that both the forward and the reverse reactions (i.e., potassium transfers from water to organic and from organic to water) produce steady-state voltammetric responses. If the potassium concentration in the aqueous phase is much higher than the crown ether concentration in DCE, both limiting IT currents (i.e., from the outer solution into the pipet and from the filling solution out of the pipet) are determined by spherical diffusion of either DB18C6 or [K^+DB18C6] in the external organic solution. Therefore, facilitated IT reaction 1 yields true steady-state voltammograms at micrometer- or nanometer-sized pipets. In contrast, simple IT, e.g., the transfer of TEA^+,

$$TEA^+ (DCE) \rightarrow TEA^+(w) \qquad (2)$$

involves spherical diffusion in the outer liquid phase, as well as diffusion of TEA^+ inside the narrow shaft of a pipet, which is often described as quasi-linear. A typical micropipet voltammogram in this case consists of a sigmoidal wave that corresponds to the transfer of TEA^+ from DCE into the aqueous phase inside a pipet and a non-steady-state reverse peak. Our objective here is to show that nanopipet voltammetry allows one to study simple IT processes and yields consistent values of kinetic parameters for both forward and reverse reactions.

Experimental Section

Chemicals. The following materials were used as-received: tetrabutylammonium chloride (TBACl), potassium tetrakis(4-chlorophenyl) borate (KTPBCl), dibenzo-18-crown-6 (DB18C6), tetraethylammonium chloride (TEACl), trimethylchlorosilane, and 1,2-dichloroethane (DCE, 99.8%, HPLC grade) from Aldrich (Milwaukee, WI); tetramethylammonium chloride (TMACl) from Fluka; and sodium tetraphenylborate (NaTPB) from J. T. Baker (Phillipsburg, NJ). Tetrahexylammonium perchlorate ($THAClO_4$) from Johnson Matthey (Ward Hill, MA) was recrystallized twice from an ethyl acetate/ether (9:1) mixture and was dried under vacuum overnight at room temperature, according to the literature procedure.[24] Tetramethylammonium tetrakis(4-chlorophenyl)borate (TMATPBCl), tetraethylammonium tetrakis(4-chlorophenyl)borate (TEATPBCl), and tetrabutylammonium tetrakis(4-chlorophenyl)borate (TBATPBCl) were prepared via the metathesis of KTPBCl and TMACl, TEACl, or TBACl, respectively, as described previously.[25] Tetrahexylammonium tetraphenylborate was precipitated from $THAClO_4$ and NaTPB and recrystallized three times from acetone.[15b] All aqueous solutions were prepared from deionized water (Milli-Q, Millipore Corp., Bedford, MA).

Nanopipet Preparation. The pipets (with radii of 10−300 nm) were made either from borosilicate capillaries (outer diameter/inner diameter (OD/ID) ratio of 1.0/0.58) or quartz capillaries (length of 10 cm, OD/ID = 1.0/0.70) from Sutter Instrument Co. (Novato, CA), using a laser-based pipet puller (P-2000, Sutter Instrument Co.), as described previously.[12a,19,26] Two halves of the same pulled capillary yield a pair of almost identical micropipets with the same orifice radius. Several pulling programs were developed to produce short (patch-type) pipets from quartz and borosilicate glass. The pipets were filled with aqueous solution from the rear, using a small (10−25 μL) syringe. A Ag/AgCl reference was inserted into each pipet from the rear. All prepared pipets were inspected using an Olympus BH2 optical microscope (at magnifications of 100× to 500×).

In some experiments (see below), the outer glass wall of a pipet was silanized to render it hydrophobic. This was done by dipping the pipet tip into trimethylchlorosilane for 3−5 min while the flow of argon (sufficiently fast to produce small bubbles) was passed through the pipet from the back to avoid silanization of the inner pipet wall. This was crucial because the external organic solvent gets drawn inside a pipet if its inner surface is hydrophobic.

Instrumentation and Procedures. A BAS 100B electrochemical workstation (Bioanalytical Systems, West Lafayette, IN) and an EI-400 four-electrode potentiostat (Ensman Instruments, Bloomington, IN) were used to record the cyclic voltammograms. Voltammetric experiments with pipets were performed in a U-type cell inside a Faraday cage. The voltage was applied between two reference electrodes, both of which were 0.25- or 0.125-μm-diameter silver wires (Aldrich) that were coated with AgCl. All experiments were conducted at room temperature (23 ± 2 °C).

SECM experiments were performed using an instrument described previously.[13a,b] The approach curves were obtained in a DCE-filled Teflon cell. A 3-mm-diameter glassy carbon electrode (BAS) that was inserted through the bottom of the cell served as a substrate. The organic reference electrode was prepared by coating a silver wire with silver tetrakis(4-chlorophenyl)borate (AgTPBCl) via anodization in DCE solution that contained 10 mM TBATPBCl. Before the measurements, the pipet was positioned above the substrate and biased at a potential where the IT process was diffusion-limited. The approach curves were obtained by moving the tip toward the substrate and recording the tip current as a function of separation distance.

Results and Discussion

Characterization of Nanopipets by Voltammetry and SECM. Knowledge of the nanopipet size and shape is essential for extraction of the kinetic parameters from the voltammetric

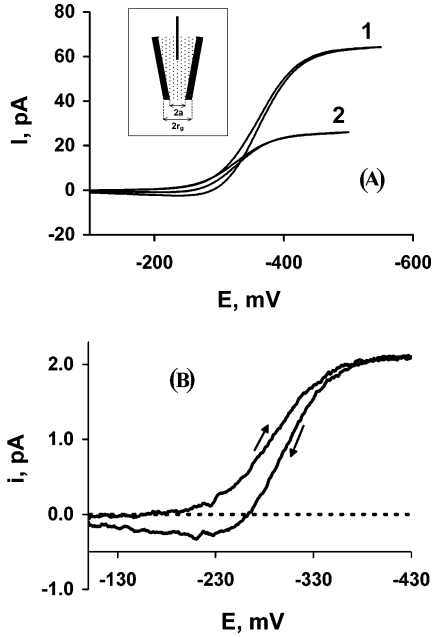

Figure 1. (A) Cyclic voltammograms of TEA^+ transfer across a DCE/water interface formed at (curve 1) nonsilanized and (curve 2) silanized nanopipets of the same radius (124 nm). (B) Background-subtracted voltammogram at the 10-nm-radius silanized pipet. The potential sweep rate was 20 mV/s. For other parameters, see cell 1. The inset in panel A shows a schematic diagram of a pipet electrode.

data.[1d] To determine whether the procedures developed earlier for the silanization of micrometer pipets are also suitable for nanopipets, we investigated the effect of silanization on the diffusion-limiting current of IT reactions 1 and 2. Two typical voltammograms of the TEA^+ transfer from DCE into the aqueous filling solution inside the pipet (Figure 1A) were obtained in the following cell:

Ag|AgCl|10 mM NaTPB + 10 mM NaCl||
aqueous reference solution

0.4 mM TEATPBCl + 0.01 M THATPB||
outer DCE solution

10 mM LiCl|AgCl|Ag (cell 1)
pipet

Curve 1 in Figure 1 was obtained before silanization, and the orifice radius (a = 124 nm) was calculated from eq 3:[22]

$$i_p = 3.35\pi nFaDc \quad (3)$$

where D and c are the diffusion coefficient and concentration of TEA^+ in DCE, respectively, a is the inner pipet radius, F is the Faraday constant, and n is the transferred charge. Equation 3 was shown to describe the diffusion-limiting current to a nonsilanized pipet correctly.[19,22]

Curve 2 in Figure 1A was obtained at a silanized pipet, which was otherwise identical to that used to produce curve 1. The height of the steady-state wave decreased markedly after the silanization. The diffusion-limiting current to a silanized pipet ($i_{p,s}$) is given by eq 4:[13b,19,27]

$$i_{p,s} = AnFaDc \quad (4)$$

The factor A is dependent on the pipet wall thickness as follows:[28]

$$A = 4.0000 + 4B(\mathrm{RG} - C)^D \quad (5)$$

TABLE 1: Effect of Silanization on the Steady-State Diffusion Limiting Current of TEA^+ Transfer from DCE into Water-Filled Borosilicate Nanopipets

a (nm)[a]	i_p (pA)	$i_{p,s}$ (pA)	$i_p/i_{p,s}$
265	102.1	46.4	2.20
219	67.7	38.2	1.77
211	83.4	37.0	2.26
148	57.6	25.8	2.23
133	66.2	23.3	2.84
124	53.7	21.7	2.47
68	31.1	11.8	2.63
25	12.0	4.4	2.71
10	3.5	1.7	2.09

[a] Calculated from eq 4 with $A = 4.64$, $D_{TEA^+} = 9.76 \times 10^{-6}$ cm^2/s, and $c_{TEA^+} = 0.4$ mM.

where $B = 0.1380$, $C = 0.6723$, $D = -0.8686$, and RG is the ratio of the radius of the pipet glass sheath to the orifice radius (RG = r_g/a).

Comparing eqs 3 and 4, one can see that the ratio of the limiting currents for nonsilanized and silanized pipets of the same radius ($i_{p,s}/i_p$) should be between 2.0 (for RG = 1.1) to 2.6 (for RG = 10). Thus, the successful silanization of the outer pipet wall should decrease the limiting current by a factor of 2.0−2.6. The ratio of the plateau currents extracted from curves 1 and 2 ($i_p/i_{p,s} = 2.4$) corresponds to an RG value of ~2.

The shape of the steady-state voltammograms can be further improved by background subtraction,[12a] which diminishes the effects of the double-layer charging current and of parallel charge-transfer processes across the ITIESs. The background curve is recorded with the same pipet electrode in a DCE solution of the same composition, but with no transferred ion present. An example of a background-subtracted voltammogram of TEA^+ transfer is shown in Figure 1B. This curve consists of a steady-state wave, corresponding to the transfer of TEA^+ from DCE into the aqueous phase inside a pipet, and a non-steady-state reverse peak. The latter is due to quasi-linear diffusion of TEA^+ inside the pipet. Despite the very small size of the pipet (radius of 11 nm), the low current (≤2 pA), and the minor distortions caused by digital subtraction, the voltammogram in Figure 1B is well-shaped and suitable for kinetic analysis.

A more-extensive set of background-subtracted voltammograms at silanized and nonsilanized pipets (Table 1) yielded an average $i_p/i_{p,s}$ value of 2.3. This corresponds to $A = 4.6$, or RG = 1.6 (from eq 5). Although the calculated RG values were similar for a large number of different pipets (as one would expect when similar capillaries and the same pulling program are used), the pipet geometry characterization would be more reliable if the a and RG values could be determined independently by a different technique. Our nanopipets were too small ($a \ll 1$ μm) to examine the tip using optical microscopy; thus, we used SECM to evaluate a and RG. Figure 2 shows how the pipet shape parameters can be extracted from an SECM approach curve. The current across the micro-ITIESs was produced by the IT of potassium from water to DCE, facilitated by DB18C6 (reaction 1) in the following cell:

Ag|AgTPBCl|0.25 mM DB18C6 + 10 mM TBATPBCl||
outer DCE solution

100 mM KCl|Ag|AgCl (cell 2)
pipet

The experimental I_T vs d/a curve (where I_T is the tip current normalized by the $i_{p,s}$ value measured in the bulk solution) in Figure 2 was obtained with a pipet tip that had a radius of 290

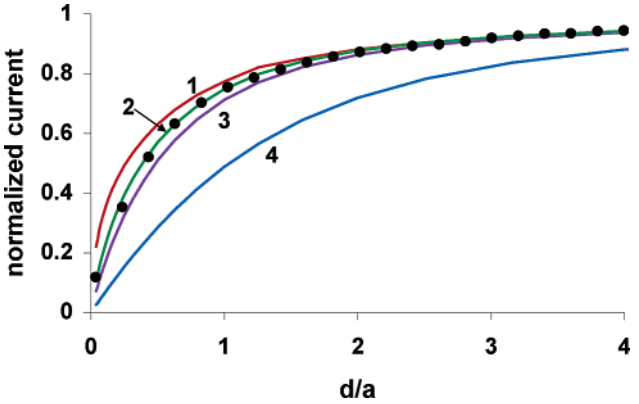

Figure 2. Experimental (symbols) and theoretical (solid lines) scanning electrochemical microscopy (SECM) current−distance curves for facilitated K^+ transfer from water to DCE at a 290-nm pipet approaching a solid substrate. Theoretical curves are calculated for a = 290 nm, and RG = 1.1 (curve 1), 1.5 (curve 2), 2.0 (curve 3), and 10 (curve 4), using analytical approximations from ref 13b.

nm. The ratio of the diffusion-limiting current at that pipet before and after silanization was consistent with RG = 1.5. As the tip approached the glassy carbon substrate, the tip current decreased because the diffusion of DB18C6 to the pipet orifice was hindered by the solid surface. Four theoretical approach curves (solid lines) in Figure 2 were calculated using previously published analytical approximations[13b] for different RG values (from 1.1 to 10). The fitting procedure showed that the radius value is really not an adjustable parameter, and a good fit can be obtained only for a specific radius value. The experimental data in Figure 2 fits the theoretical curve for RG =1.5 well. In contrast, the curvatures of the I_T vs d/a dependences calculated for RG = 1.1 or RG = 2.0 are significantly different. The curve calculated for RG =10 is so different that no reasonable fit between it and the experimental data is possible. The RG value for the pipet in Figure 2 can be evaluated as RG = 1.5 ± 0.3. This range is in an excellent agreement with the average RG value of 1.6 that is determined from the voltammograms of several pipets (see Table 1), as well as with the OD/ID ratio of the used borosilicate capillaries (1.0/0.58 = 1.7). Thus, the value of RG = 1.5 and the corresponding value of A = 4.64 (from eq 4) will be used for the kinetic analysis of voltammograms obtained at borosilicate pipets (see below). A very good fit between the experimental and theoretical approach curves with the tip current decreasing to ~10% of the bulk value at the shortest tip/substrate separation distance suggests that the liquid/liquid nano-interface is essentially flat and not recessed (i.e., DCE does not get inside the pipet).

The effectiveness of quartz pipet silanization was also examined using reaction 1 as a source of steady-state current, and the results were somewhat different from those obtained with borosilicate nanopipets. The average decrease in the diffusion-limiting current after silanization, $i_p/i_{p,s}$, was ~1.5, i.e., lower than the theoretically expected value. This finding indicates that the protocol used for the borosilicate pipets does not result in complete silanization of a quartz pipet surface and, therefore, does not completely remove an aqueous film from its outer wall. Our experiments with micrometer-sized pipets (for which both the orifice radius and the RG value could be determined microscopically) confirmed the aforementioned finding: the diffusion-limiting current after 3 min of silanization of a quartz pipet exceeded the expected value (calculated using microscopically measured value of a and RG) by ~50%. After longer (e.g., 6 min) silanization, the measured diffusion-limiting currents agreed with the theoretical values. However, there is always a possibility of partial blocking of the nanopipet orifice, as a result of excessively long silanization.[13e] Because the kinetic parameters obtained with silanized and nonsilanized pipets are typically similar (see below), it may be safer not to perform long silanization for steady-state voltammetric measurements with quartz nanopipets.

TABLE 2: Kinetic Parameters for Facilitated Transfer of Potassium with DB18C6 at Nonsilanized (1−7) and Silanized (1s−7s) Quartz Nanopipets

pipet number	a (nm)	$\Delta E_{1/4}$ (mV)	$\Delta E_{3/4}$ (mV)	α	$k°$ (cm/s)	$E°$ (mV)
1	150.2	33.1	34.7	0.56	0.3	215
1s	150.2	34.7	39.3	0.34	0.48	242
2	147.2	32.4	35.5	0.42	0.5	244
2s	147.2	33.2	34.2	0.53	0.55	248
3	106.1	34.5	38.7	0.44	0.48	241
3s	106.1	40.1	46.27	0.29	0.54	249
4	89.5	33.9	40.9	0.32	0.8	243
4s	89.5	31.5	33.6	0.44	0.8	245
5	87.5	38.7	45.9	0.27	0.71	250
5s	87.5	34.2	38.7	0.37	0.96	253
6	75.5	31.6	33.4	0.36	1.19	207
6s	75.5	33.2	35.5	0.57	1.62	200
7	67.5	30.1	36	0.42	0.86	241
7s	67.5	35.5	36.3	0.34	1.53	223

The effect of silanization on kinetic parameter values obtained from nanopipet voltammograms was investigated for facilitated potassium transfer. Assuming uniform accessibility of liquid/liquid interface formed at the pipet tip, the standard rate constant ($k°$) and charge-transfer coefficient (α) can be determined by fitting an experimental voltammogram to the following theoretical equation:[29]

$$\frac{i}{i_d} = \frac{1}{1 + \exp[\alpha nf(E - E^{0'})]/\lambda + (m_f/m_r)\exp[\alpha nf(E - E^{0'})]} \quad (6)$$

where m_f and m_r are the mass-transfer coefficients for the species whose diffusion controls the rate of the forward and reverse IT reaction, respectively, $m_f/m_r = 1.6$,[12a] $\lambda = k°/m_f$, $f = F/(RT)$, E is the applied interfacial voltage, and i_d (= i_p or $i_{p,s}$) is the diffusion-limiting current. To determine the m_f value, which is required for calculating the rate constant, one must know the pipet radius. For silanized pipets, a was determined from eq 4 with A = 4.64, and $m_f = i_d/(\pi F a^2 c)$. For nonsilanized pipets, the true interfacial area is not known. To find the rate constant, we used the notion of the equivalent hemisphere, i.e., a uniformly accessible interface, the current to which would be equal to the current to the given pipet. Using the equivalent hemisphere radius (r), the mass-transfer coefficient can be calculated as $m_f = i_d/(2\pi F r^2 c)$.

The kinetic parameters of reaction 1 obtained at silanized and nonsilanized quartz pipets in cell 2 are summarized in Table 2. Two different approaches—the fitting of the experimental voltammogram to the theory and the three-point method based on the measurements of the half-wave potential ($E_{1/2}$) and two quartile potentials ($E_{1/4}$ and $E_{3/4}$)[29]—were used to extract kinetic parameters from steady-state voltammograms. The values obtained by the two methods were similar, and only those coming from the fit are presented in the table. As discussed previously, the three-point method provides two useful diagnostic criteria, based on easily accessible values of $\Delta E_{1/4} = |E_{1/4} - E_{1/2}|$ and $\Delta E_{3/4} = |E_{1/2} - E_{3/4}|$: (i) reliable values of kinetic parameters can only be obtained if $\Delta E_{1/4} \geq$ 30.5 mV and $\Delta E_{3/4}$

≥ 31 mV (otherwise, the voltammogram is essentially Nernstian); and (ii) the inequality $\Delta E_{3/4} \geq \Delta E_{1/4}$ holds true for any undistorted quasi-reversible voltammogram. These criteria are useful because the shape of the experimental steady-state voltammogram may be distorted and may not suitable for kinetic analysis, even if its fit to the theory seems to be satisfactory.[12a] Here, and below, the kinetic parameters were extracted only from voltammograms that satisfied both criteria.

The mean values of the standard rate constant and transfer coefficient found from the voltammograms at silanized pipets (see Table 2) are $k^\circ = 0.9 \pm 0.4$ cm/s and $\alpha = 0.4 \pm 0.1$. (Here, and below, the uncertainties shown are 95% confidence intervals.) The mean rate constant value obtained using nonsilanized pipets is slightly lower ($k^\circ = 0.7 \pm 0.2$ cm/s); however, the difference is within the range of experimental error. The transfer coefficient value found with nonsilanized pipets is essentially the same as that obtained after silanization ($\alpha = 0.40 \pm 0.07$). Both α values are in perfect agreement with the results reported in ref 12a. Both k° values are slightly lower than that determined in ref 12a and are very similar to that obtained in ref 13d.

Measurements of Simple Ion Transfer (IT) Kinetics Using Nanopipets: TEA^+ and TMA^+ Transfers from Dichloroethane (DCE) to Water. It is commonly assumed that the sigmoidal wave of simple IT at a micropipet-based ITIES, which is due to spherical diffusion of the ions to the pipet orifice in the external solution, can be treated as a steady-state voltammogram.[30] Accordingly, the nanopipet voltammograms of TEA^+ transfer from DCE to water obtained at silanized nanopipets in cell 1 were observed to be in an excellent agreement with eq 6 (Figure 3). The theoretical fit in Figure 3 is shown only for the forward wave. No exact theory is available for the reverse (non-steady-state) wave, because the geometry of the pipet inside is uncertain and probably complicated. The kinetic parameters of IT reaction 2, which were obtained with pipets of different sizes and various TEA^+ concentrations, are summarized in Table 3. The mean value of $k^\circ = 2.1 \pm 0.2$ cm/s is significantly higher than all values reported previously for TEA^+ transfer; however, it is only slightly higher than $k^\circ = 1.3$ cm/s, which was measured using nanopipets for K^+ transfer across the DCE/water interface facilitated by DB18C6.[12a] Both k° and the transfer coefficient ($\alpha = 0.70 \pm 0.04$) are essentially independent of TEA^+ concentration and pipet radius (see Table 3).

Using the same approach, we measured the kinetic parameters of TMA^+ transfer across the DCE/water interface, which is supposed to be slightly slower than the TEA^+ transfer. The experiments were performed in cell 3:

$$\begin{array}{c} \text{Ag|AgCl|10 mM TBACl ||} \\ \text{aqueous reference solution} \end{array}$$

$$\begin{array}{c} x \text{ mM TMATPBCl} + \text{10 mM TBATPBCl||} \\ \text{outer DCE solution} \end{array}$$

$$\begin{array}{c} \text{10 mM LiCl|Ag|AgCl} \\ \text{pipet} \end{array} \qquad \text{(cell 3)}$$

where $x = 0.2$, 0.4, or 0.8.

The results shown in Table 4 are similar to the TEA^+ case, in terms of the rate constant and transfer coefficient values ($k^\circ = 1.5 \pm 0.3$ cm/s and $\alpha = 0.60 \pm 0.04$), as well as the absence of a strong correlation between the measured values and either the pipet radius or the TMA^+ concentration.

Kinetics of TEA^+ Transfer from Water to DCE. Despite self-consistency of the aforementioned kinetic measurements, the validity of the steady-state analysis of simple IT voltammograms is not obvious. Equation 6 is based on an assumption that all three consecutive steps of the process (i.e., diffusion of TEA^+ in the outer DCE solution, interfacial IT, and diffusion of TEA^+ in the aqueous filling solution inside the pipet) occur at the same rate. However, quasi-linear diffusion inside the pipet narrow shaft is a non-steady-state process, as evidenced by the presence of a current peak in Figure 1B. Such a peak was always present in our voltammograms that were obtained with borosilicate nanopipets. Because the rate of non-steady-state diffusion inside a pipet is time-dependent, it cannot always be equal to the rate of steady-state spherical diffusion to the pipet orifice. This observation casts some doubt on the applicability of eq 6

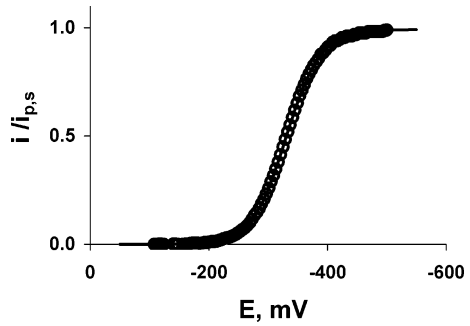

Figure 3. Background-subtracted steady-state voltammogram (symbols) of TEA^+ transfer from DCE to water at a 25-nm-radius silanized pipet and the best theoretical fit (solid line, calculated from eq 6). For other parameters, see cell 1.

TABLE 3: Kinetic Parameters for TEA^+ Transfer from DCE into Water-Filled Silanized Borosilicate Nanopipets

c_{TEA^+} (mM)	a (nm)	α	k° (cm/s)
0.2	110	0.79	1.41
0.2	82	0.77	2.23
0.2	65	0.67	2.59
0.2	96	0.63	2.13
0.4	126	0.72	1.81
0.4	133	0.64	1.92
0.4	148	0.74	1.81
0.4	105	0.70	1.51
0.4	125	0.79	1.86
0.4	78	0.63	1.80
0.4	72	0.77	2.31
0.4	68	0.78	2.01
0.4	42	0.81	2.69
0.4	15	0.81	2.70
0.8	127	0.69	1.89
0.8	108	0.58	2.37
0.8	101	0.62	2.42
0.8	99	0.59	2.45

TABLE 4: Kinetic Parameters for TMA^+ Transfer from DCE into Water-Filled Nanopipets

c_{TEA^+} (mM)	a (nm)	α	k° (cm/s)
0.2	223	0.50	0.95
0.2	150	0.62	1.19
0.2	91	0.54	1.65
0.4	218	0.56	0.88
0.4	210	0.61	0.88
0.4	193	0.47	1.11
0.4	170	0.50	1.23
0.4	144	0.63	1.89
0.4	141	0.67	1.94
0.4	115	0.72	1.93
0.4	110	0.69	1.90
0.4	83	0.64	2.60
0.4	19	0.59	2.80
0.8	257	0.69	0.86
0.8	177	0.50	1.10

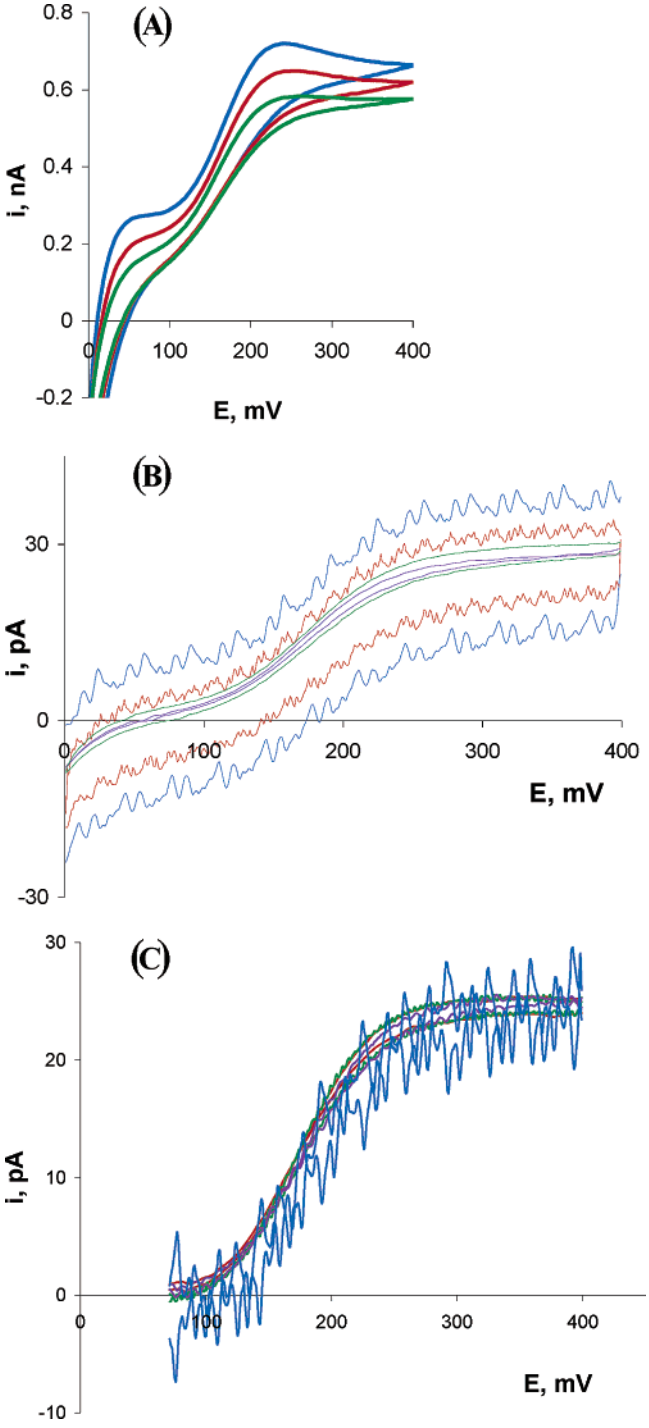

Figure 4. Cyclic voltammograms for TEA^+ transfer from the pipets filled with an aqueous phase to outer DCE solution using cell 4. The TEACl concentration in the filling solution was 0.25 mM. The pipet radius was (A) 1 μm and (B and C) 80 nm. In panel A, the scan rate υ (in mV/s) was 20 (green), 50 (red), and 100 (blue); in panel B, υ (in mV/s) was 20 (purple), 100 (green), 1000 (red), and 2000 (blue). Panel C shows the voltammograms after background subtraction for υ (mV/s) = 50 (purple), 100 (green), 200 (red), and 2000 (blue).

to kinetic analysis of data in Table 3 and compelled us to probe the reverse IT reaction

$$TEA^+(w) \rightarrow TEA^+(DCE) \qquad (7)$$

Previously, it was shown[12a] that the length of the narrow shaft has a tendency to somewhat decrease as the pipet radius decreases (this corresponds to a larger inner angle at the pipet tip) resulting in a lower than expected resistance of nanopipets. By optimizing our pulling programs, we obtained even shorter quartz nanopipets whose internal resistances were lower than the values reported in ref 12 for similar pipet radii. The narrow shaft of such a pipet is apparently sufficiently short to observe steady-state, quasi-spherical diffusion inside it.[31] To contrast the steady-state and non-steady-state situations, Figure 4 shows two series of voltammograms of TEA^+ transfer from the aqueous filling solution to the outer, DCE liquid phase obtained in cell 4:

$$\underset{\text{aqueous reference}}{Ag|AgCl|10\ mM\ TBACl}||\underset{\text{outer DCE solution}}{10\ mM\ TBATPBCl}||\underset{\text{pipet}}{10\ mM\ LiCl + 0.25\ mM\ TEACl}|AgCl|Ag \qquad \text{(cell 4)}$$

The curves in Figure 4A were obtained with a 1-μm-radius pipet. They exhibit a well-defined peak whose height grows as the scan rate increases, in agreement with previous reports.[30] In contrast, the voltammograms of the same IT process obtained with an 80-nm pipet (Figure 4B) are completely sigmoidal, even at a scan rate (υ) as fast as 2 V/s. The shape of these curves is essentially independent of υ, except for higher charging current and oscillations observed at faster scan rates. The similarity of these voltammograms becomes apparent after the background subtraction (Figure 4C) and confirms the quasi-steady-state nature of the IT from short nanopipets to an external solution. After background subtraction, these voltammograms exhibit almost perfect shapes, suitable for kinetic experiments (Figure 5).

The analysis of the voltammograms (Table 5), based on eq 6, yielded kinetic parameters of $k° = 2.3 \pm 0.5$ cm/s and $\alpha =$

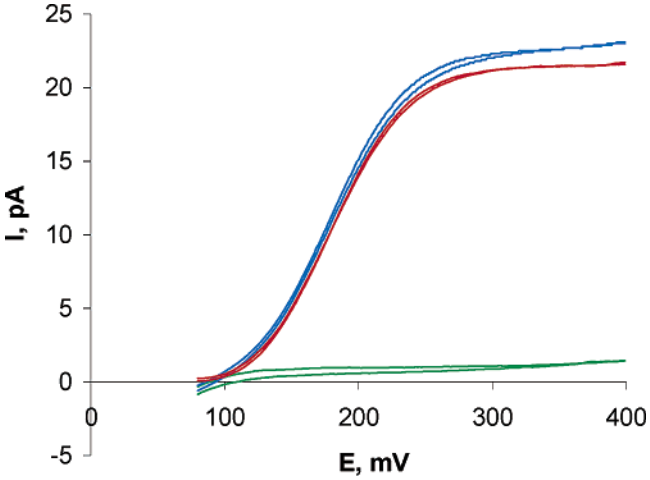

Figure 5. Voltammograms of TEA^+ transfer from water to DCE. The TEACl concentration in the filling solution was 0.25 mM; a = 80 nm and υ = 20 mV/s. The red curve was obtained by subtracting the background voltammogram (green) from the original voltammogram (blue) and correcting for the 1.1 pA current offset.

TABLE 5: Kinetic Parameters for TEA^+ Transfer from Water to DCE[a]

a (nm)	$k°$ (cm/s)	α	$E°$ (mV)
123.0	1.1	0.44	158.7
102.9	1.6	0.44	161.8
89.0	2.4	0.71	171.2
88.3	2.7	0.68	160.4
80.3	2.6	0.56	166.2
70.0	1.8	0.81	163.6
69.1	3.5	0.81	171.2
65.0	2.7	0.45	163.2

[a] $[TEA^+] = 0.25$ mM.

0.6 ± 0.1 for reaction 7. The standard potential value extracted from the fit was essentially constant. An excellent agreement has been observed between the k° values obtained for the forward IT (reaction 2) and reverse IT (reaction 7) of TEA^+. However, the sum of two transfer coefficients ($\sim$1.3) is somewhat higher than the theoretically expected value (1.0).

The large measured values of the IT rate constants can be discussed within the frame of the slow interfacial diffusion model in which the standard rate constant is defined as[5]

$$k^\circ = \frac{D_i}{\Delta x}$$

where D_i and Δx are the diffusion coefficient within the boundary layer and the thickness of that layer, respectively. Assuming values of $\Delta x \approx 1$ nm and $k^\circ = 2$ cm/s, one obtains $D_i = 2 \times 10^{-7}$ cm^2/s. The latter value, although significantly smaller than the diffusion coefficient of TEA^+ in either water or DCE, is not as strikingly low as $D_i = 10^{-8}$ cm^2/s, the value corresponding to $k^\circ \approx 0.1$ cm/s, which has been commonly used to check the theory.[7]

Conclusions

The kinetic parameters for two rapid simple ion transfer (IT) reactions—the transfers of tetraethylammonium (TEA^+) and tetramethylammonium (TMA^+) ions between dichloroethane (DCE) and water—were measured under steady-state conditions, using nanometer-sized pipets. Essentially the same value of the standard rate constant (2.1−2.3 cm/s) was obtained for the forward (from DCE to water) and reverse (from water to DCE) transfer of TEA^+, which may be the fastest IT process studied to date. The results provide a justification for the use of quasi-steady-state voltammograms of IT from short nanopipets to external solution for kinetic analysis.

Similar to micrometer-sized pipets, the outer wall of a water-filled nanopipet immersed in organic solvent is covered with a thin aqueous layer. The silanization methodology developed for micropipets[19] is also effective for the removal of an aqueous film from the outer wall of a nanopipet that is made of borosilicate glass. This procedure, combined with background subtraction, allows one to achieve quantitative agreement between the experimental and theoretical values of diffusion current to the nanopipet. The complete silanization of quartz nanopipets requires more exposure time and should be done cautiously to avoid precipitation of a thick film that can partially block the pipet orifice.

The shape parameters (i.e., the orifice radius and the ratio of the glass wall radius to the orifice radius of a nanopipet used as an SECM tip can be obtained from analysis of the current−distance curve. The pipets used as SECM tips must be silanized to obtain an acceptable fit between the theory and the experiment. However, the differences between kinetic parameters obtained from steady-state voltammetry at silanized and non-silanized nanopipets are typically within the range of experimental error.

Acknowledgment. The support of this work by the National Science Foundation (CHE-0315558 and INT-0003774) and a grant from PSC-CUNY are gratefully acknowledged. Our thanks to François Laforge, Dr. Wenju Feng, and Prof. Takashi Kakiuchi for technical assistance and helpful discussions.

References and Notes

(1) For recent reviews of ion transfer reactions at the ITIES, see the following: (a) Girault, H. H. In *Modern Aspects of Electrochemistry*, Vol. 25; Bockris, J. O'M., Conway, B. E., White, R. E., Eds.; Plenum Press: New York, 1993; p. 1. (b) Samec, Z.; Kakiuchi, T. Charge Transfer Kinetics at Water-Organic Solvent Phase Boundaries. In *Advances in Electrochemical Science and Electrochemical Engineering*, Vol. 4; Gerischer, H., Tobias, C. W., Eds; VCH: New York, 1995; p. 297. (c) Benjamin, I. *Annu. Rev. Phys. Chem.* **1997**, *48*, 401. (d) Liu, B.; Mirkin, M. V. *Electroanalysis* **2000**, *12*, 1433.

(2) (a) Reymond, F.; Fermín, D.; Lee, H. J.; Girault, H. H. *Electrochim. Acta* **2000**, *45*, 2647. (b) Vanysek, P. *Trends Anal. Chem.* **1993**, *12*, 357. (c) Gennis, R. B. *Biomembrances*; Springer: New York, 1995.

(3) Gurevich, Y. Y.; Kharkats, Y. I. *J. Electroanal. Chem.* **1986**, *200*, 3.

(4) Schmickler, W. *J. Electroanal. Chem.* **1997**, *426*, 5.

(5) (a) Kakiuchi, T. *J. Electroanal. Chem.* **1992**, *322*, 55. (b) Kontturi, K.; Manzanares, J. A.; Murtomaki, L.; Schiffrin, D. J. *J. Phys. Chem.* **1997**, *101*, 10801.

(6) Dang, L. X. *J. Phys. Chem. B* **2001**, *105*, 804.

(7) Marcus, R. A. *J. Chem. Phys.* **2000**, *113*, 1618.

(8) Benjamin, I. *J. Chem. Phys.* **1992**, *97*, 1432.

(9) Nagatani, H.; Fermín, D. J.; Girault, H. H. *J. Phys. Chem. B* **2001**, *105*, 9463.

(10) (a) Taylor, G.; Girault, H. H. *J. Electroanal. Chem.* **1986**, *208*, 179. (b) Campbell, J. A.; Girault, H. H. *J. Electroanal. Chem.* **1989**, *266*, 465.

(11) Beattie, P. D.; Delay, A.; Girault, H. H. *Electrochim. Acta* **1995**, *40*, 2961.

(12) (a) Shao, Y.; Mirkin, M. V. *J. Am. Chem. Soc.* **1997**, *119*, 8103. (b) Yuan, Y.; Shao, Y. *J. Phys. Chem. B* **2002**, *106*, 7809.

(13) (a) Shao, Y.; Mirkin, M. V. *J. Electroanal. Chem.* **1997**, *439*, 137. (b) Shao, Y.; Mirkin, M. V. *J. Phys. Chem. B* **1998**, *102*, 9915. (c) Selzer, Y.; Mandler, D. *J. Phys. Chem. B* **2000**, *104*, 4903. (d) Sun, P.; Zhang, Z.; Gao, Z.; Shao, Y. *Angew. Chem., Int. Ed.* **2002**, *41*, 3445. (e) Li, F.; Chen, Y.; Sun, P.; Zhang, M.; Gao, Z.; Zhan, D.; Shao, Y. *J. Phys. Chem. B* **2004**, *108*, 3295.

(14) Gavach, C.; d'Epenoux, B.; Henry, F. *J. Electroanal. Chem.* **1975**, *64*, 107.

(15) (a) Samec, Z.; Mareček, V. *J. Electroanal. Chem.* **1986**, *200*, 17. (b) Wandlowski, T.; Mareček, V.; Holub, K.; Samec, Z. *J. Phys. Chem.* **1989**, *93*, 8204. (c) Wandlowski, T.; Mareček, V.; Samec, Z.; Fuoco, R. *J. Electroanal. Chem.* **1992**, *331*, 765. (d) Mareček, V.; Lhotský, A.; Račinský, S. *Electrochim. Acta* **1995**, *40*, 2909. (e) Lhotský, A.; Holub, K.; Neužil, P.; Mareček, V *J. Chem. Soc., Faraday Trans.* **1996**, *92*, 3851.

(16) (a) Kakiuchi, T.; Noguchi, J.; Kotani, M.; Senda, M. *J. Electroanal. Chem.* **1990**, *296*, 517. (b) Kakiuchi, T.; Noguchi, J.; Senda, M. *J. Electroanal. Chem.* **1992**, *336*, 137.

(17) Kakiuchi, T.; Teranishi, Y. *J. Electroanal. Chem.* **1995**, *396*, 401.

(18) Rahman, Md. A.; Doe, H. *J. Electroanal. Chem.* **1997**, *424*, 159.

(19) Shao, Y.; Mirkin, M. V. *Anal. Chem.* **1998**, *70*, 3155.

(20) (a) Tokuda, K.; Kitamura, F.; Liao, Y.; Okuwaki, M.; Ohsaka, T. In *Charge Transfer at Liquid/Liquid and Liquid/Membrane Interface*; Kyoto, 1996; pp 7−8. (b) Liao, Y.; Okuwaki, M.; Kitamura, F.; Ohsaka, T.; Tokuda, K. *Electrochim. Acta* **1998**, *44*, 117.

(21) Samec, Z.; Lhotský, A.; Mareček, V. *Electrochim. Acta* **1999**, *45*, 583.

(22) Beattie, P. D.; Delay, A.; Girault, H. H. *J. Electroanal. Chem.* **1995**, *380*, 167.

(23) Amemiya, S.; Bard, A. J. *Anal. Chem.* **2000**, *72*, 4940.

(24) Tsionsky, M.; Bard, B. J.; Mirkin, M. V. *J. Am. Chem. Soc.* **1997**, *119*, 10785.

(25) Shao, Y.; Girault, H. H. *J. Electroanal. Chem.* **1990**, *282*, 59.

(26) Wei, C.; Bard, A. J.; Feldberg, S. W. *Anal. Chem.* **1997**, *69*, 4627.

(27) Shoup, D.; Szabo, A. *J. Electroanal. Chem.* **1984**, *160*, 27.

(28) Zoski, C. G.; Mirkin, M. V. *Anal. Chem.* **2002**, *74*, 1986.

(29) Mirkin, M. V.; Bard, A. J. *Anal. Chem.* **1992**, *64*, 2293.

(30) Stewart, A. A.; Taylor, G.; Girault, H. H.; McAleer, J. *J. Electroanal. Chem.* **1990**, *296*, 491.

(31) Tong, Y.; Shao, Y.; Wang, E. *Anal. Chem.* (in Chin.) **2001**, *11*, 1241.